Synthesis and characterisation of Ureido-pyrimidinone based supramolecular conducting polymer nanocomposite for fabrication of electrochemical devices

T.V.Rajendran[1], V.Jaisankar[1]*, E.K.T.Sivakumar[2]

[1]**PG and Research Department of Chemistry Presidency College, Chennai-05, Tamilnadu, (INDIA)**
[2]**Centre for Nano science&Technology, Anna University, Chennai-25, Tamil Nadu, (INDIA)**
E-mail: vjaisankar@gmail.com

ABSTRACT

This paper describes the preparation and characterisation of Ureido-pyrimidinone based supramolecular polymer/ferrite nanocomposites for electrochemical applications. The synthesized supramolecular polymer is blended with ferrite nanoparticles by dispersion method which is used as an energy storage material in electrochemical devices. The structural property of composite was studied by X-ray diffraction method (XRD). The structure of the repeating units in the supramolcular polymer, ferrite and nanocomposite was studied by FTIR spectroscopy. The morphology of substrate was studied by Scanning electron microscopy (SEM). The electrical conductivity measurements such as AC conductivity, dielectric constant and dielectric loss were evaluated at different frequencies (1 kHz to 1 MHz) using Electron Impedance Spectroscopy (EIS). The effect of temperature on the ionic conductivity of the nanocomposite was studied. It is observed that the ionic conductivity is maximum for supramolecular polymer nanocomposite. Further, the results showed that increase in dielectric constant as a function of frequency indicates an increase in AC conductivity.   © 2015 Trade Science Inc. - INDIA

KEYWORDS

Ferrite nanocomposite;
Dielectric constant;
Supramolecular polymer;
SEM.

INTRODUCTION

In recent years, polymer nanocomposites containing ferrite nanoparticles are under intense research because of their unique structural, thermal and electrical properties[1-3]. Nanocomposite polymers are an active area of study in material science. They are prepared by complexing polymers containing hydrogen bonds with ferrite nanoparticles. Being light weight, these materials are used as solid polymer electrolytes in solid-state electrochemical devices such as batteries, fuel cells and electrochemical displays[4-8]. Polymer electrolytes usually contain both crystalline and amorphous phases. Supramolecular polymer contains nitrogen atom in its structure and interact with ferrites for movement of

Full Paper

ions from polymer to ferrite nanoparticles[9]. In general, ferrite nanoparticles are prepared by co-precipitation method using metal chloride and ferric chloride as raw materials in presence of alkaline medium[10]. Zinc ferrite is a good sample of the relation between nanoparticle structure, composition and properties[11,12]. Among recent research articles concerned with polymer-blended magnetic materials, Varshney et al., reported an approach to synthesise nano-stick shaped ferromagnetic iron oxide/polypyrrole, which influenced the properties of polypyrrole and controlled morphology of Fe_2O_3, that lead to form stick-shaped polymer composites decorated with Fe_2O_3 nanoparticles[13-15]. This phenomenon resulted in the formation of conducting/ferromagnetic/polymer nanocomposite with an electrical conductivity of the order of 10^{-2} S/cm, which prove the attractive feature of polymer-blended magnetic materials and showed that polymers are good additive to ferrites[16]. In addition, zinc ferrite containing composites have been shown to exhibit an enhanced magneto-optical and a large magneto-electric effect[17].

In the present work, supramolecular functionalised polymeric ferrite nanocomposites have been synthesized and characterised by various techniques such as FT-IR, XRD method, SEM, Thermal and impedance analysis. The supramolecular polymer contains hydrogen bonds can interact with metal oxide present in the ferrite nanoparticles. The formation of H-Metal-O bonds in the supramolecular polymer metal nanocomposites with high ionic conductivity is one the main objectives in polymer research. This is because of their applications as electrolytes in solid-state batteries, electrochemical display devices/smart windows, photo electrochemical cells etc., due to their high conductivity, high energy density, wide range electrochemical stability and easy processability.

EXPERIMENTAL METHODS

Materials

Zinc chloride ($ZnCl_2$), Iron chloride

($FeCl_3.6H_2O$) and NaOH were purchased from Merck; Poly (ethylene glycol) (PEG) was purchased from SD Fine chemicals; 2-amino-4-hydroxy-6-methylpyridine, 2,4-diisocyanato toluene and dibutyl tin dilaurate (DBTDL) were purchased from Aldrich. PEG was dried at 60^oC for 24 hrs and 2-amino-4-hydroxy-6-methylpyrimidine was dried at 70^oC for 6 hrs before synthesis. Chloroform, DMF and Hexane were dried using common drying agents, distilled and stored prior to use.

Procedure

Synthesis of UPy based supramolecular polymer

The UPy synthon was synthesized by donor-acceptor H bonding between isocyanate and pyridine groups and it was reported in our previous investigation[18]. Poly (ethylene glycol) (PEG) (5g) was dissolved in dry chloroform (50 ml), DBDTL (2 drops), and then UPy synthon (2.5g) was added and heated with stirring for 20 hours. Then, the reaction mixture was stirred overnight at room temperature. The solvent was partially evaporated under reduced pressure. Then, the resulting material was precipitated from chloroform in hexane and filtered. The white material obtained was dried for 2 days under reduced pressure.

Synthesis of $ZnFe_2O_4$ nanoparticles

The zinc ferrite nanoparticles were prepared by co-precipitation method[19]. Ferric chloride and zinc chloride solutions with Fe to Zn in the ratio 2:1 are taken beaker containing 100ml of distilled water. To this 50ml aqueous solution of 1.5 M NaOH was added in drops with constant stirring at 90^oC for 2 hours. The resultant precipitate formed and it was collected and centrifuged at 3000 rpm and then washed with distilled water and acetone for several times and finally dried, at 100^oC for 6 h.

Synthesis of UPy based supramolecular polymer nanocomposites

The supramolecular/ferrite nanocomposite was prepared by mixing the stochiometric amount of (1:0.2) synthesised supramolecular polymer and $ZnFe_2O_4$ nanoparticles in 30 ml of distilled water at

room temperature with constant stirring for 2 hrs. The ferrite nanoparticles are uniformly distributed in the polymer matrix and the solvent was evaporated by drying under reduced pressure. The resulting supramolecular polymer –magnetic ferrite nanocomposite was dried at room temperature for an additional 6 h and is utilized for further characterization and applications.

Characterisation

The synthesized supramolecular polymer ferrite nanocomposites was characterised by the X-ray diffraction pattern using GEOL JDX-8P X-ray diffractometer having Cu Kα (0.154 nm) radiation to generate diffraction patterns from powder crystalline samples at ambient temperature in a 2θ range of 20° to 90°. Fourier transformed infrared (FT-IR) spectra were measured in transmission mode with a Perkin Elmer model-4000 FT-IR infrared spectrometer in the range 400-4000 cm^{-1}. Thermal behavior of the samples was examined by simultaneous differential scanning calorimeter/ thermogravimetric analysis (DSC/TGA, model STA 1640) in air at the heating rate of 20°C/min. The morphology of the nanocomposite sample was determined by using scanning electron microscope (SEM model LEICA S430). The real (ε') and imaginary (ε'') parts of nanocomposite dielectric permittivity and AC conductivity have been calculated over a wide range of temperatures (30°C and 100°C) and at frequencies 10 and 100 kHz using dielectric-impedance analyser.
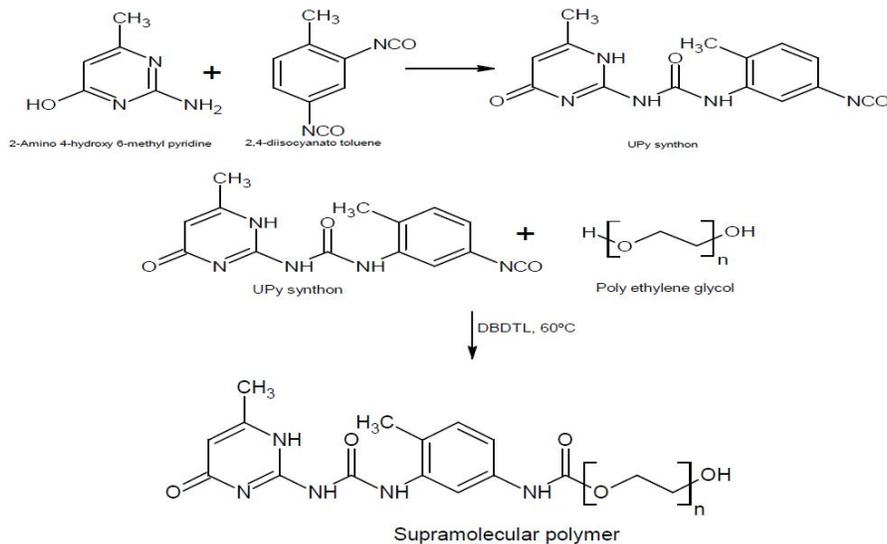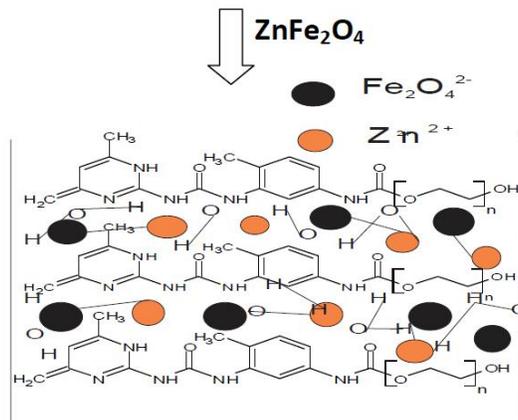
Figure 1 : Synthesis scheme of polymer/ferrite nanocomposite at room temperature

Full Paper

RESULTS AND DISCUSSION

Synthesis scheme of supramolecular polymer/ferrite nanocomposite

The supramolecular polymer and it composite was synthesised by the following reaction scheme at room temperature,

FT-IR analysis

The IR spectra recorded for supramolecular polymer, ferrite nanoparticles and supramolecular polymer ferrite nanocomposites are shown in Figure 2. The peak at 3338 cm^{-1} indicates the NH stretching of secondary amine. The peak at 1366 cm^{-1} is assigned to C-N stretching of the benzene ring. The peaks at 3612 and 2927 cm^{-1} indicates the stretching and bending vibration of O-H and C-H bonds respectively. Two absorption bands at 561 and 470 cm^{-1} corresponding to the Fe-O stretching modes of tetrahedral and octahedral sites as expected from normal spinal structure[20,21].
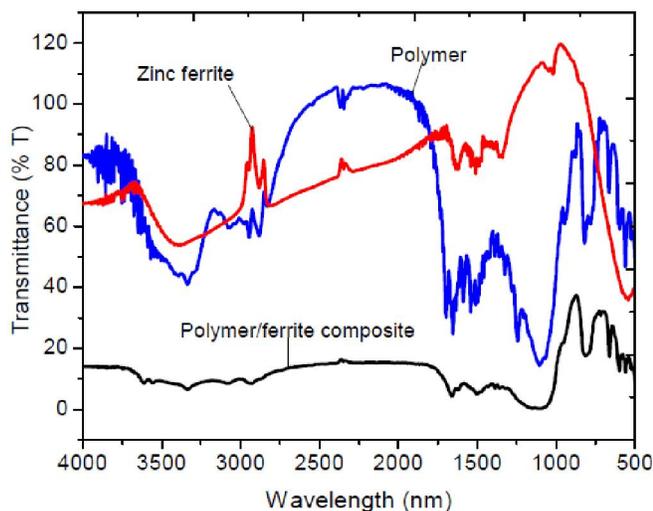
Figure 2 : FT-IR spectra of supramolecular polymer, zinc ferrite nanoparticle and polymer/ ferrite nanocomposite

XRD analysis

The synthesized zinc ferrite nanoparticles and supramolecular polymer ferrite nanocomposites were characterized by X-ray diffraction method. Figure 3(a) and (b) shows XRD pattern of ferrite and polymer/ferrite nanocomposites respectively. The XRD peaks appeared in the diffractogram confirms the spinel structure of the synthesized ferrite

nanocomposites (JCPDS Card No. 82-1049). XRD line broadening is used to estimate the average grain size of the nanocomposites according to Scherrer's formula:

$$D=0.9\lambda/\beta\ cos\theta$$

Where D is the average diameter of the grains, λ is the wavelength of the X-ray, θ is the Bragg's angle and β is the full width half maximum (FWHM) of the broadening peak from XRD pattern. The results showed an average crystalline size of supramolecular polymer nanocomposites was calculated as 95.2 nm. The X-ray diffractogram of the composite containing zinc ferrite nanoparticles showed a remarkable reduction in the intensity of XRD peaks. This can be attributed to a destruction effect of the ferrites
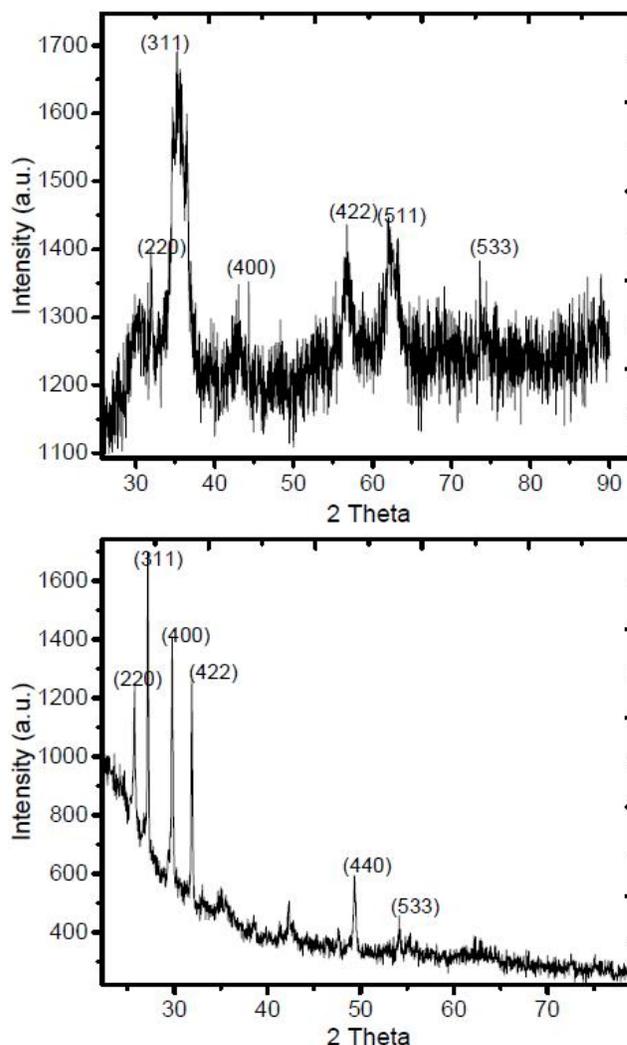
Figure 3 : (a) and (b) XRD pattern of ferrite nanoparticles and polymer ferrite nanocomposites

Full Paper
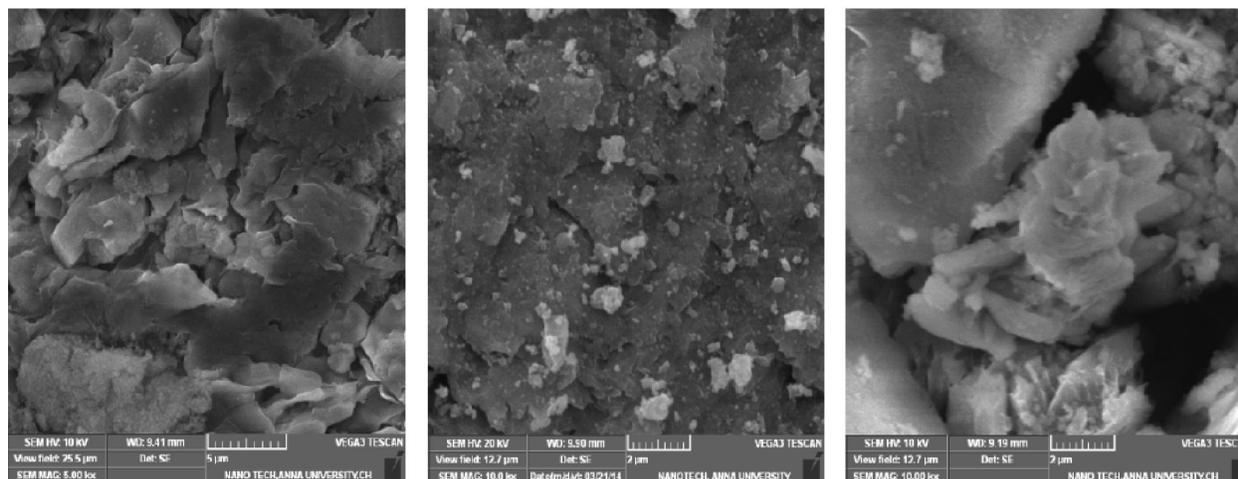
Figure 4 : (a), (b) and (c) SEM morphology of polymer, ferrite and polymer ferrite nanocomposites respectively
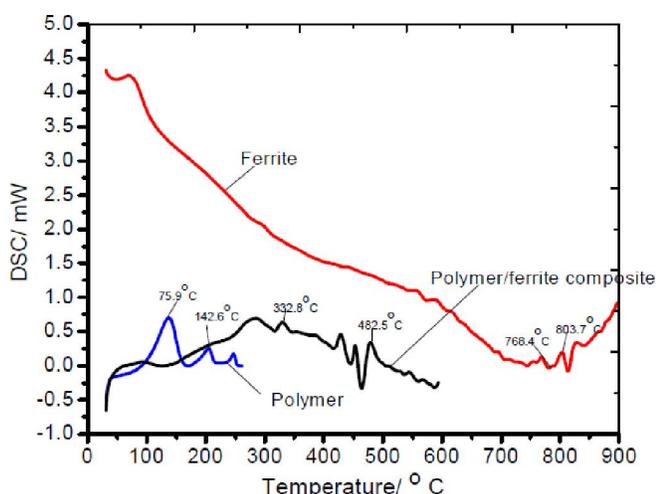
Figure 5 : DSC thermogram of supramolecular polymer, ferrite and polymer ferrite nanocomposite

on the ordered arrangement of the polymer matrix which results in, an enhancement in the crystalline phase as reported by Sui, Y.P., et al.

SEM analysis

The scanning electron microscopy (SEM) image of the supramolecular polymer, ferrite nanoparticles and supramolecular polymer nanocomposites shown in Figure 4(a)-(c) respectively. It is observed that the grain size is small and not fully growth in Figure 4(a). There is observable difference between Figures 4(b) and 4(c) in grain morphology. Thus, the above discussion confirms the formation of supramolecular polymer ferrite nanocomposites. The addition of zinc ferrite nanoparticles into supramolecular polymer, the ferrite nanoparticles did not agglomerate and they were

nearly uniform in shape, as shown in Figure 4(c). The SEM image shows that the average sizes of zinc ferrite nanoparticles are in the range between 63nm and 78nm which are in the close agreement with the XRD data.

Thermal analysis

Thermal analysis was performed to analyse the thermal stability of the synthesised supramolecular polymer, ferrite and polymer ferrite nanocomposite. Figure 5 shows DSC thermogram and is attributed to the grain growth of polymer ferrite nanocomposites. The exothermic peak at the onset temperature of around 482.5°C in the DSC thermogram corresponds to the crystallization of the synthesized polymer ferrite nanocomposites. The microstructure and atomic configuration of nanoparticles change when exposed to high temperature since the free energy of these particles is higher than that of crystalline polymer nanocomposites.

Electrical conductivity measurements

The values of equivalent parallel capacitance (Cp), dissipation factor (D), phase angle (δ) and parallel equivalent resistance (Rp) that are recorded for supramolecular polymer ferrite composite by the LCR meter at selected frequency range (f). The ac conductivity (σ_{ac}), dielectric constant (ε') and dielectric loss (tanδ) parameters have been calculated from the above values.

AC conductivity

Full Paper
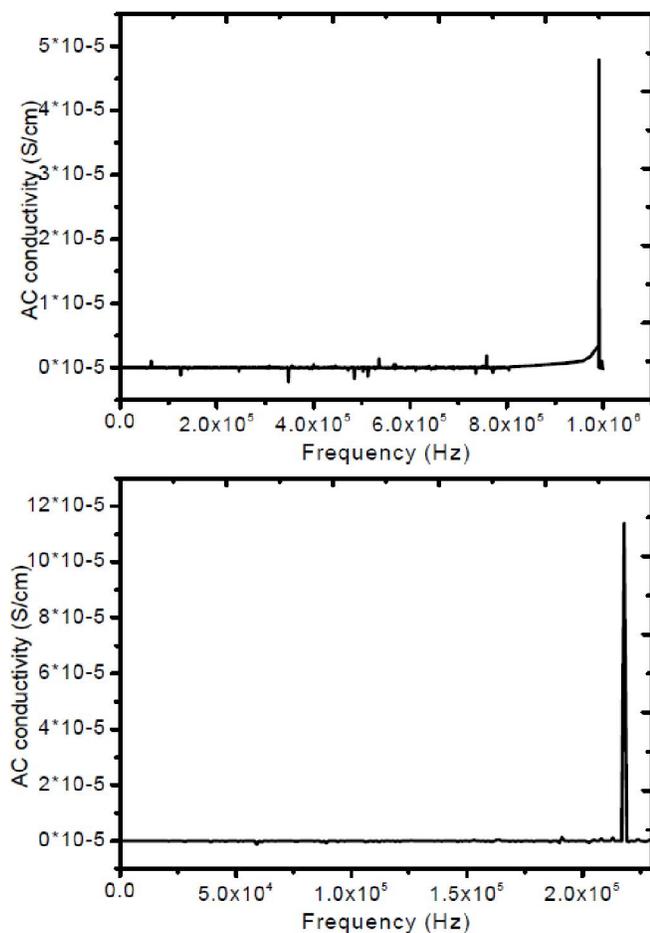
Figure 6 : (a) and (b) variation of AC conductivity of nanocomposites as a function of frequency at 30ºC and 100ºC

Figure 7 : (a) and (b) variation of dielectric constant of nanocomposites as a function of frequency at 30ºC and 100ºC

The resistance ρ_{ac} of the sample was calculated using the equation $\rho_{ac} = Rp \times A/t$ where Rp is the resistance of the nanocomposite was determined from the intercept of the impedance spectrum on the Z' real axis, t is the thickness of the polymer nanocomposite and A is the surface area. The conductivity σ_{ac} was determined using the formula $\sigma_{ac} = 1/\rho_{ac}$ The calculated ionic conductivity of nanocomposites values are 4.63×10^{-5} S/cm and 11.23×10^{-5} S/cm at 30ºC and 100ºC respectively.

Dielectric constant

The variation of real permittivity (ε') of supramolecular polymer nanocomposites as a function of frequency shown in Figure 6 (a) and (b) at 30ºC and 100ºC respectively. It is observed that the dielectric constant decreases with increase in frequency for the nanocomposites, as frequences increases dielectric constant decreases. The strong frequency dispersion of permittivity is observed in the low frequency region followed by a nearly frequency independent behavior above 10 kHz.

Dielectric loss

Figure 8(a) and (b) shows a variation of dielectric loss of supramolecular polymer nanocomposites as a function of frequency at 30ºC and 100ºC respectively. The high value of dielectric constant of the polymer ferrite nanocomposites may be explained on the basis of the structural changes associated with the ferrite nanoparticles when the size is reduced to nanometer scale.
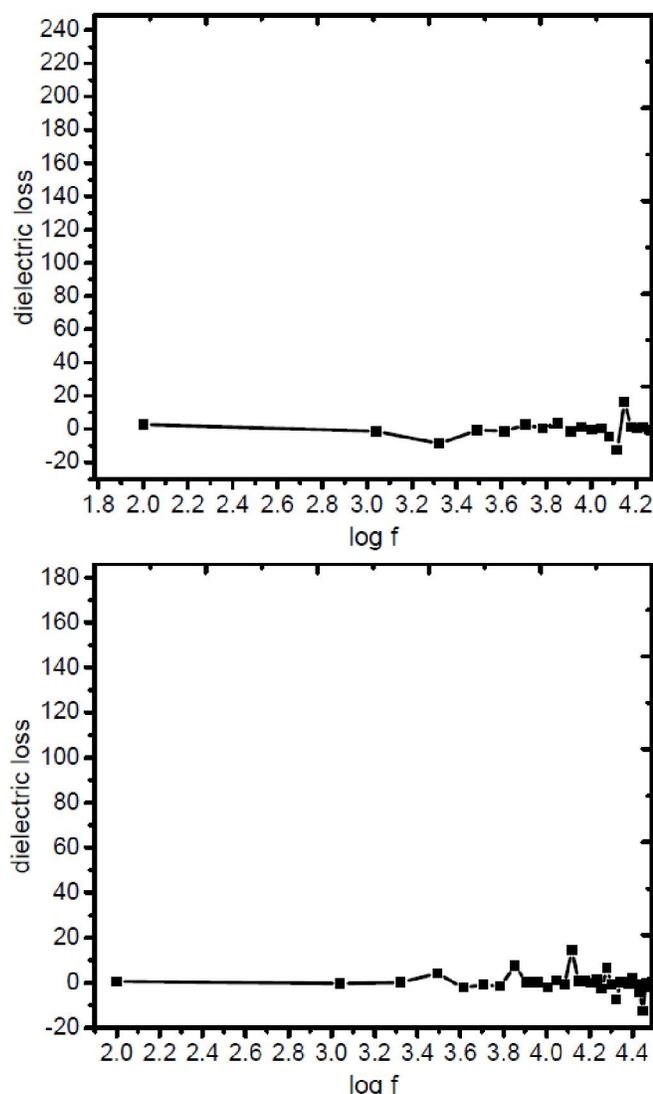
Figure 8 : (a) and (b) variation of dielectric loss of nanocomposites as a function of frequency at 30ºC and 100ºC

thermogravimetric differential scanning calorimetry (TG-DSC) analysis. The electrical conductivity measurements such as AC conductivity, dielectric constant and dielectric loss were measured using electronic impedance spectroscopy (EIS) analysis. The highest conductivity value of ferrite nanocomposite is 11.23×10^{-5} S/cm at 100ºC which shows the thermal stability of the synthesized nanocomposites at high temperature. The results indicate that the synthesized supramolecular polymer ferrite nanocomposite is useful for the fabrication of new generation electrical devices.

CONCLUSION

In this investigation, Ureido-pyrimidinone based supramolecular polymer ferrite nanocomposite was prepared by incorporation of ferrite nanoparticles into the polymer matrix by dispersion method. The crystalline size of ferrite nanoparticles was calculated by XRD technique and the diffractogram shows the agglomeration of ferrite nanoparticles in the polymer composites. The surface morphology was characterized by using SEM analysis. The crystalline nature of ferrite nanocomposites was found by using

REFERENCES

[1] M.Dariel, L.H.Bennett, D.S.Lashmore, P.Lubitz, M.Rubinstein, W.L.Lechter, M.Z.Harford; J.Appl.Phys., **61**, 4067 (**1987**).

[2] R.Guo, L.Fang, W.Dong, F.Zheng, M.Shen; J.Phys.Chem., **114**, 21390 (**2010**).

[3] Y.Hakuta, H.Ura, H.Hayashi, K.Arai; Ind.Eng.Chem.Res., **44**, 840 (**2005**).

[4] A.K.Thakur, S.A.Hashmi; Solid State Ionics., **181**, 1270-1278 (**2010**).

[5] R.N.Mason, L.Hu, D.T.Glatzhofer, R.Frech; Solid State Ionics., **180**, 1626-1632 (**2010**).

[6] R.C.Agarwal, Y.K.Mahipal, R.Ashrafi; Solid State Ionics., **192**, 6-8 (**2011**).

[7] P.L.Kuo, W.J.Liang, T.Y; Chen Polymer., **44**, 2957-2964 (**2003**).

[8] L.S.Ng, A.A.Mohammed; Journal of Power Sources., **163**, 382-385 (**2006**).

[9] S.L.Agarwal, M.Singh, M.Tripathi, M.M.Dwivedi, K.Pandey; Journal of Materials Science., **44**, 6060-6068 (**2009**).

[10] P.Sivakumar, R.Ramesh, A.Ramanand; Mater le., **65**, 483-485 (**2011**).

[11] Y.Li, R.Yi, A.Yan, L.Deng, K.Zhou, X.Liu; Solid State Sci., **11**, 1319 (**2009**).

[12] M.Gharagozlou; J.Alloys Compd., **486**, 660 (**2009**).

[13] S.Varshney, K.Singh, A.Ohlan, V.K.Jain, V.P.Dutta, S.K.Dhawan; J.Alloys Compd., **538**, 107-114 (**2012**).

[14] R.M.Khafagy; J.Alloys Compd., **509**, 9849-9857 (**2011**).

[15] R.M.Khafagy; Curr.Nanosci., **8**, 375-386 (**2012**).

[16] Y.Xiaowei, Z.Yanwai, C.Tongxiang, H.Zhenxing;

Full Paper

Appl.Surf.Sci.*, **258**, 7365-7371 **(2012)**.

[17] J.Ryu, S.Priya, K.Uchino, H.Kim; J.Electro-ceram.*, **8**, 10 **(2002)**.

[18] T.V Rajendran, V.Jaisankar; J.of Polymer composites.*, **3**, 1 **(2014)**.

[19] P.Sivakumar, R.Ramesh, A.Ramanand; Mater Lett., **65**, 483-485 **(2011)**.

[20] A.Baykal, N.Kasapoglu, Y.Koseoglu, A.C.Basaran, H.Kavas; Cent.Eur.J.Chem., **6**, 125 **(2008)**.

[21] N.Kasapoglu, A.Baykal, Y.Koseoglu, M.S.Toptak; Scripta Materialia., **57**, 441 **(2007)**.